

# Rapid determination of renal filtration function using an optical ratiometric imaging approach

Weiming Yu, Ruben M. Sandoval, and Bruce A. Molitoris

Nephrology Division, Department of Medicine, Indiana University School of Medicine, Indianapolis, Indiana

Submitted 14 June 2006; accepted in final form 14 February 2007

**Yu W, Sandoval RM, Molitoris BA.** Rapid determination of renal filtration function using an optical ratiometric imaging approach. *Am J Physiol Renal Physiol* 292: F1873–F1880, 2007. First published February 20, 2007; doi:10.1152/ajprenal.00218.2006.—Glomerular filtration rate (GFR), which measures the amount of plasma filtered through the kidney within a given time, is an essential and clinically important indicator of kidney function. Here, we report a new ratiometric measurement technique based on intravital fluorescence microscopy that allows rapid evaluations of renal function in rodent models. By using this technique, plasma clearance rates of a fluorescent GFR marker can be measured in less than 5 min following a bolus infusion of a fluorescent dye mixture into the bloodstream. The plasma clearance kinetics of the GFR marker showed consistent values when measured in healthy animals at locations both in the kidney and from the skin. In addition, by using this technique, we were able to rapidly determine renal function with acute renal failure animal models and with other animal models where kidney filtration functions were altered. The measured plasma clearance kinetics using this technique correlated with expected changes in kidney function. We found this ratiometric approach offers improved accuracy and speed for quantifying renal function compared with the approach using single fluorescent probes, and the measurement can be done noninvasively from the skin. This approach also offers a high sensitivity for determining plasma clearance rate of a fluorescent compound. This feature is important for rapidly quantifying small differences in plasma clearance when kidney function is changing.

GFR; plasma clearance rate; intravital microscopy; ischemia; acute renal failure; two-photon excitation; dextran; multiphoton

DEVELOPMENT OF INTRAVITAL microscopy has opened up new windows for studying the kidney (6, 13–15), the associated disease processes (12, 22–24), and molecular trafficking and metabolism (19, 26). Following an intravenous infusion of fluorescent dye molecules, one can monitor processes such as apoptosis and necrosis of tubular cells, vascular permeability defects, abnormal blood flow patterns and glomerular filtration of molecules with different sizes with regard to kidney injuries by performing intravital kidney imaging (7, 13, 23). A wealth of information can be retrieved from analysis of these *in vivo* images. It is apparent that to understand the dynamic processes of the kidney, quantitative analysis of *in vivo* images is essential. Recently, we have developed a ratiometric imaging technique by using the generalized polarity concept for quantitative analysis of multicolor fluorescence images and demonstrated its potential power for detecting relative concentration changes of multiple probes both spatially and temporally (28, 29). The filtration property of a glomerulus and specific reabsorptive characteristics of a tubular section for different fluo-

rescent molecules are among those of particular interests that can be quantified. We began to address important questions specifically related to glomerular permselectivity or tubular reabsorption by using this quantitative approach (29). What is unique about imaging intact tissues from live animals vs. isolated tissues or cell culture models is the ability to access the kinetics of different biological processes systemically within local tissues. Here, we report a technique that allows rapid measurement of plasma clearance rates of a particular molecule and glomerular filtration rate (GFR) using intravital microscopy.

The gold standard of determining GFR is via measurement of plasma clearance of a marker molecule that can be filtered freely through the glomerular filtration barrier, not protein bound or metabolized, and is not reabsorbed. Inulin is one good example and an often used GFR marker. Results based on plasma clearance using a single injection of inulin, or other marker molecules, correlate well in patient tests (5, 8). Techniques applying plasma clearance allow rapid determination of GFR in both normal patients as well as patients with acute renal failure (ARF) in a matter of ~15 min (5, 17, 18). This is an attractive advantage for assessing renal function of ARF patients over methods requiring a multiple-hour period of urine collection that are not applicable in these patients. This imaging technique we developed and tested on rodents maintains this important feature for rapid determination of kidney filtration function.

It has been previously reported that by using a fluorescent marker molecule, such as FITC-inulin, following a single bolus injection, GFR can be determined by measuring plasma clearance kinetics based on fluorescence intensity decay (16). The measured results correlated well with renal functions under various controlled experimental conditions where the kidney function was known to change (16). When animal models with superficial glomeruli are used, glomerular filtration can be visualized with two-photon excitation microscopy at near real-time speeds (28) and subsequently single-nephron GFR (snGFR) can be measured when fluorescent GFR markers were used (9). So far, these fluorescence techniques for measuring GFR are all based on the quantification of fluorescence intensity values from a single fluorescence source. It is understandable that measurements using intensity values alone, from a single source, are subject to errors caused by experimental conditions such as ambient light, fluctuations from excitation light source, and the high-voltage supply of the detectors. The fluorescence intensity value can be further affected by the nonuniformity of the imaging detector and intensity attenuation at different

Address for reprint requests and other correspondence: W. Yu, Indiana Univ. School of Medicine, Dept. of Medicine, Nephrology Div., 950 W. Walnut St., R2-268, Indianapolis, IN 46202 (e-mail: wmyu@iupui.edu).

The costs of publication of this article were defrayed in part by the payment of page charges. The article must therefore be hereby marked “advertisement” in accordance with 18 U.S.C. Section 1734 solely to indicate this fact.

imaging depths (3). The measurement technique we report here is based on the use of two fluorescent molecules and the ratio between their intensity values. Using intensity ratioing, the ratio values are much less sensitive to signal fluctuations caused by environmental and experimental conditions (28). Most importantly, as we will discuss later, applications of intensity ratio techniques result in better defined kinetic curves of plasma clearance and improved accuracy for determining the rate constants of the marker molecules.

## MATERIALS AND METHODS

**Animal preparation.** Experimental procedures using animals were approved by the Institutional Animal Care and Use Committee and performed in accordance with the *Guide for the Care and Use of Laboratory Animals* (Washington, DC: National Academy Press, 1996). Male Sprague-Dawley rats (6–8 wk, Harlan, Indianapolis, IN), ~250 g in body weight, were used. Animals were anesthetized with an intraperitoneal injection of thiobutabarbital (130 mg/kg, Sigma, St. Louis, MO), shaved, and placed on a homeothermic table to maintain the body temperature at 37°C. After adequate anesthesia was ensured, a femoral venous catheter was placed using a 27-gauge cannula for injection of fluorescent dye solutions. One of the kidneys was exteriorized for microscopy imaging via a 10- to 15-mm lateral incision made dorsally under sterile conditions (6). The surgical procedure was only to exteriorize the kidney. Kidney blood flow was not interrupted during surgery, except when we deliberately occluded blood flow to model renal ischemic injury. For studies in which kidney ischemia was induced, the renal artery and vein were occluded with a nontraumatic microaneurysm clamp for 30 min. For studies in which the whole kidney nephrectomy was performed, the renal artery and vein were first ligated with a nonabsorbable no. 2 (metric size) silk suture before the kidney/kidneys were removed. For studies in which bilateral ureteral ligations were performed, both the left and right ureters were ligated with no. 2 silk sutures each at two points to ensure that there was no urine flow. During all procedures, core body temperature of the animal was maintained at 37°C by using a homeothermic table and monitored with a rectal thermometer.

**Fluorescent probes.** The fluorescent solution we used for intravenous injection included mixtures of 1) FITC-inulin (3–5 kDa, Sigma) and 500-kDa Texas red-dextran and 2) 3-kDa tetramethylrhodamine (TMR)-dextran and 500-kDa FITC-dextran. FITC-inulin was dissolved in 0.9% saline and dialyzed overnight to remove unbound fluorescent molecules (1-kDa cutoff). The 3-kDa TMR-dextran, 500-kDa FITC-dextran, and 500-kDa Texas red-dextran were purchased from Invitrogen (Eugene, OR) and used directly by dissolving in 0.9% saline.

**Fluorescence microscopy.** A 0.5-ml saline solution containing 3.2 mg FITC-inulin (3–5 kDa) and 1.6 mg 500-kDa Texas red-dextran was infused through the femoral venous catheter immediately before microscopic imaging. Live images of the animal organ were captured with a two-photon laser scanning fluorescence microscope system (Bio-Rad MRC-1024MP, Hercules, CA). The external detectors were used for acquiring fluorescence signals from 500 to 550 nm (green channel for FITC-inulin) and 560–650 nm (red channel for Texas red-dextran), respectively. A water-circulation heating pad was placed on the microscope stage to preheat it to 37°C. The exposed kidney of the animal was held in a 50-mm diameter tissue culture dish with a no. 1.5 cover-glass bottom (WillCo Wells, Amsterdam, The Netherlands) for imaging. The tissue culture dish was filled with 0.9% saline to maintain the moisture of the kidney. In cases of bilateral whole kidney nephrectomy, the liver was exposed and held in the tissue culture dish for imaging. Live images of the kidney/liver were taken as functions of time for plasma clearance analysis. Baseline kidney/liver images were collected before fluorescent dye infusion to record autofluorescence signals within the tissue under investigation. Typically, we

started to collect images synchronized with dye infusion, and continuously for ~5 min at a frame rate of 1.22 s. Images at later time points were collected when needed. All intravital kidney/liver images were acquired using a ×60/1.2-NA water objective and external nonscan detectors. A Ti-sapphire laser (Spectra-Physics, Mountain View, CA) was tuned to 800 nm for excitation. The excitation laser power on the sample was attenuated to between 2 and 28 mW using neutral-density filters. During all imaging procedures, the body temperature of the animal was maintained at 37°C.

**Image data analysis.** Intensity ratio images  $R(t)$  were calculated using Meta Imaging Series (version 6, Universal Imaging, West Chester, PA) on a personal computer as follows

$$R(t) = \frac{I_{\text{small}}(t)}{I_{\text{large}}(t)} \quad (1)$$

where  $I_{\text{small}}(t)$  and  $I_{\text{large}}(t)$  are fluorescence intensities of the smaller (GFR marker) and the larger size molecules at a particular pixel of an image taken at different time points, respectively. A threshold level for each detection channel was set according to the average pixel value of an area without significant autofluorescence from images taken before dye infusion. The average pixel values of intensity ratio  $R$  from a region of blood vessel lumen (regions of interest, ROI) were exported into PSI-PLOT (version 6, Salt Lake City, UT) for analysis. The image-processing procedures were performed in an equivalent manner for all images to ensure the results were comparable.

The time series intensity ratio values of a ROI from an image time series were extracted and fit nonlinearly with the following equation using the Marquardt method (2) to retrieve the (apparent) plasma clearance rate constant  $k_A$

$$R_{\text{vessel}}(t) = A \exp(-k_A t) + C \quad (2)$$

where  $R_{\text{vessel}}(t)$  is the average pixel value of the intensity ratio from a given blood vessel lumen region extracted at different time point,  $A$  is the amplitude or the preexponential factor, and  $C$  is a constant.

## RESULTS AND DISCUSSION

Figure 1 is a montage of color-combined fluorescence intensity images of the kidney from a live and healthy male Sprague-Dawley rat. These images were taken as a function of time after a bolus intravenous infusion of a dye mixture containing FITC-inulin and 500-kDa dextran labeled with Texas red. The fluorescence intensity signal from FITC-inulin is shown in green, and the 500-kDa Texas red-dextran intensity is shown in red. At about 7.3 s after dye infusion (Fig. 1B), the fluorescence intensity was mainly from the blood vessels of the kidney. The yellowish color of the blood vessel indicates that both FITC-inulin and 500-kDa Texas red-dextran were in these blood vessels. At 12.2 s (Fig. 1C), the intensity from both dye molecules increased as a result of increased plasma concentrations of both molecules. At 24.4 s (Fig. 1D), FITC-inulin was already observed in the proximal tubule lumen (in green and indicated in Fig. 1, D and E), as a result of immediate plasma clearance (glomerular filtration) of this molecule by the kidneys. At 95.2 s (Fig. 1E), the FITC-inulin appeared to accumulate in the distal tubule lumen (in green and indicated in Fig. 1, E and F), while its concentration in the proximal tubule was decreased compared with that at 24.4 s (Fig. 1D). At the same time, there was less FITC-inulin in the bloodstream compared with that at 24.4 s. Consequently, the strength of the red color from the blood vessels increases, indicating a relative increase in the 500-kDa Texas red-dextran-to-FITC-inulin concentra-

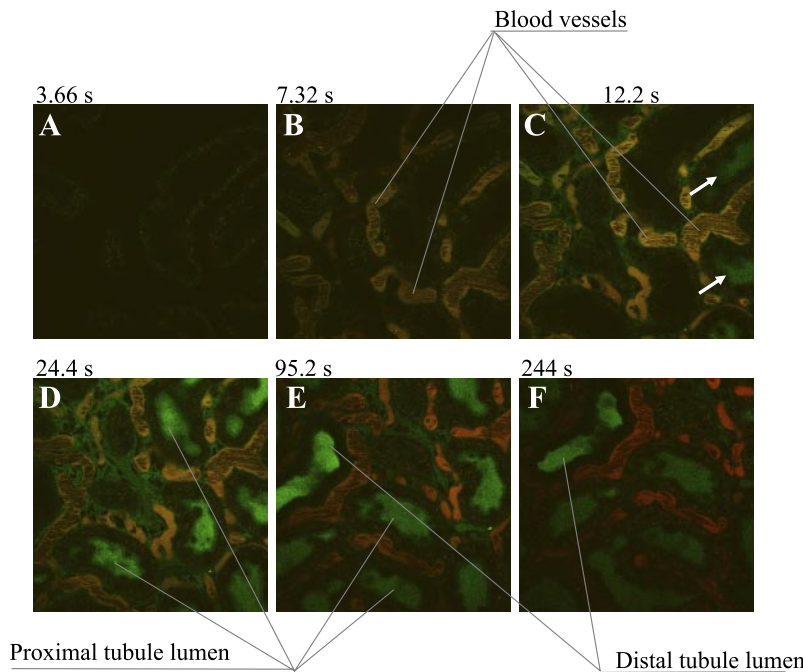


Fig. 1. Montage of color-combined fluorescence intensity time-series in vivo images of the kidney following a bolus infusion of a dye mixture. Green, FITC-inulin; red, 500-kDa Texas red-dextran. A: autofluorescence of the kidney at 3.66 s postinfusion. Dye molecules had not reached local tissue yet at this time point. As a result of glomerular filtration of FITC-inulin, it appears in both the proximal and distal tubule lumens over time (B–F), and the color of the capillary blood vessels becomes increasingly red due to plasma clearance of FITC-inulin and increased fractional concentration of the 500-kDa Texas red-dextran. The image frame size is  $200 \times 200 \mu\text{m}^2$ .

tion ratio due to plasma clearance of FITC-inulin. At 244 s (Fig. 1F), the FITC-inulin concentration continues to decrease from the bloodstream due to further clearance. This was accompanied by intensity decreases from both the proximal and distal tubule lumens (Fig. 1F). This type of time-series image collection contains dynamic information about a given molecule passing through the glomerular filtration barrier of the kidney and becoming part of the filtrate. This is the basis for measuring plasma clearance kinetics and glomerular filtration function.

To quantify the molecular filtration rate, we used the intensity ratio (Eq. 1) of the FITC-inulin and the 500-kDa Texas red-dextran (Fig. 2). The intensity ratio from the blood vessels (shown in cyan in Fig. 2) changed in time with a change of relative concentrations of the two dyes. Since the 500-kDa dextran is not cleared by the kidneys, due to its large size, it stays in the bloodstream for a very long time (days) after infusion. Typically, there is no noticeable intensity drop from the 500-kDa dextran within the time period we follow a dye infusion (anywhere between 5 and 30 min). Figure 3 is an

example of the intensity time series of the 500-kDa Texas red-dextran measured from a blood vessel, following a bolus infusion, for up to 79 min. The initial intensity spike (see inset) was due to dye injection and fast distribution of the dye molecules into the whole blood volume. There was no significant intensity drop for the rest of the curve. Effectively, the decrease in the FITC-inulin-to-500-kDa Texas red-dextran intensity ratio from the blood correlates with the concentration decrease in FITC-inulin.

In Fig. 4, we plot the FITC-inulin-to-500-kDa Texas red-dextran intensity ratio as a function of time after a bolus infusion along with the result of a least squares fit. Each data point in Fig. 4 was the average ratio value of the same region from a blood vessel extracted from an image time series (such as the images shown in Fig. 2). We plot data points every 1.22 s up to 120 s, then every 6.1 s until  $\sim 244$  s. The data had two phases (Fig. 4): the initial phase and the clearance phase (or the filtration phase/elimination phase). The signal increase of the initial phase was due to relative dye distributions and accumulations in the kidney. The highest point (at  $\sim 15$  s) of

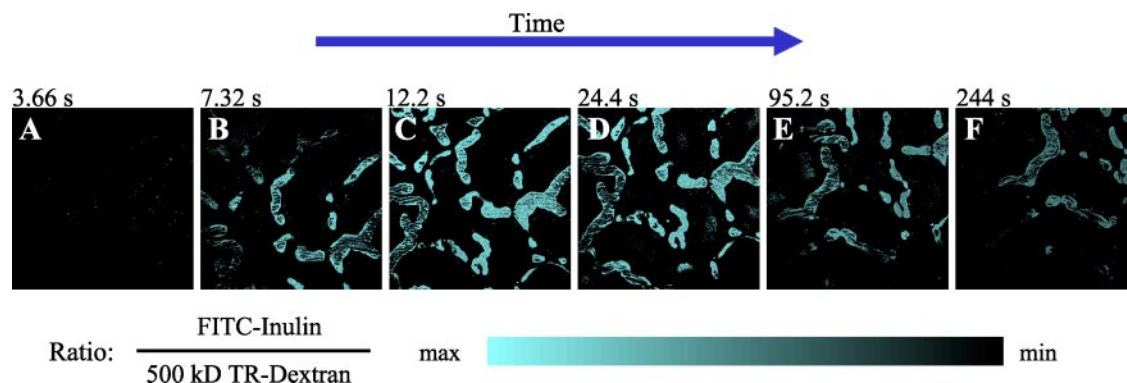


Fig. 2. Fluorescence intensity ratio images (using the same data set as in Fig. 1) of the kidney following a bolus infusion of dye mixture showing the regions of the capillary blood vessels. The decreasing of the ratio value over time is visible. The image frame size is  $200 \times 200 \mu\text{m}^2$ .

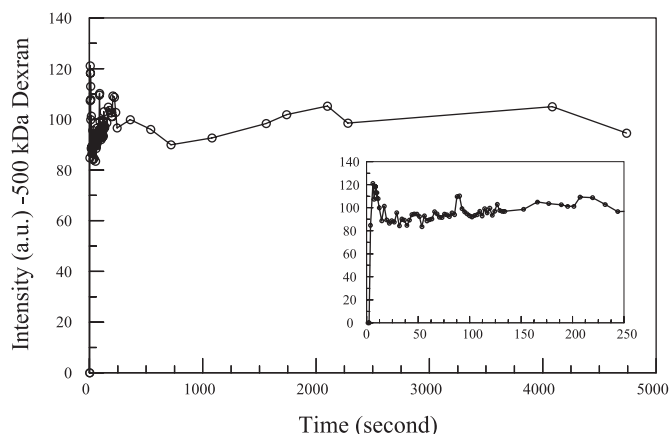


Fig. 3. Fluorescence intensity of the 500-kDa Texas Red-dextran measured from within the plasma as a function of time following a bolus infusion. *Inset*: the first 250 s after infusion. There was no significant intensity drop over the 79-min time period the intravital imaging measurements were performed.

the curve, which marks the starting point of the clearance phase, correlates with the beginning of the appearance of FITC-inulin in the proximal tubule in this case. The data points of the clearance phase fit well with a single exponential (Eq. 2). We obtained a FITC-inulin plasma clearance rate constant,  $k$  (or  $k_A$ ), of  $0.0097 \text{ (s}^{-1}\text{)}$  with  $\sim 2\%$  error (using 95% confidence limits) (2).

*Plasma clearance rates measured using various animal models.* Measurement results of plasma clearance of a single fluorescent (GFR) marker molecule have been shown to correlate with renal function (16). Using the intensity ratio of two fluorescent molecules, as in our case, should not change this fact. To prove this point and to demonstrate the capability of this ratiometric microscopic measurement technique for evaluations of abnormal kidney functions, we performed kinetic imaging experiments in a number of animal models where their GFRs were altered.

All plasma clearance rate constants plotted in Fig. 5 were measured using Sprague-Dawley rats. The clearance rate constant in Fig. 5A was measured from control animals where the kidney function was not altered. In the case of unilateral kidney ischemia (Fig. 5B), intravital microscopic images were taken from healthy kidneys of live rats. At 24 h after a 30-min unilateral kidney ischemia, the clearance rate constant was down to  $k = 0.0082 \pm 0.0002 \text{ s}^{-1}$ . This reduction of plasma clearance rate was expected (11). Significant reductions of the plasma clearance rate constants were obtained at 24 h after a 30-min bilateral kidney ischemia (Fig. 5D,  $k = 0.0035 \pm 0.001 \text{ s}^{-1}$ ). This result correlated with the blood urea nitrogen (BUN) and creatinine measurements reported in the literature using similar kidney ischemia models (10, 27).

As negative controls we measured the changes in the plasma clearance rate constant following whole-kidney nephrectomy. The reduction of the clearance rate constant measured immediately after unilateral nephrectomy (within  $<30$  min, Fig. 5C) was as expected. The nonzero rate constant after bilateral nephrectomy (Fig. 5E) indicates nonrenal “clearance” (due to nonspecific tissue distribution) of FITC-inulin that needs to be corrected for calculating the GFR (Eqs. 3 and 4; discussed in the following sections).

Bilateral ureteral ligation is an alternative way to reduce and stop glomerular filtration. Plasma clearance rate constants in Fig. 5, F–H, were measured in the same animal, at  $\sim 15$ , 60, and 90 min after bilateral ureter ligations. The clearance rate constant of the first measurement (Fig. 5F),  $\sim 15$  min after ligation, was the same as the control (Fig. 5A), indicating normal kidney function at this time point. Kidney filtration started to decrease when urine began to back up from the ureters upstream. As a result, the clearance rate constant was decreased to  $k = 0.0081 \pm 0.0016 \text{ s}^{-1}$  at 1 h (Fig. 5G) and further down to  $k = 0.0046 \pm 0.0021 \text{ s}^{-1}$  at 90 min (Fig. 5H). This rate constant is similar to those of the bilateral nephrectomy (Fig. 5E) and bilateral ischemia observations at 24 h postinjury (Fig. 5D).

*Plasma clearance rate constant vs. GFR.* The nonspecific tissue (nonrenal) distribution rate constant  $k_T$  was determined from double whole-kidney nephrectomy experiments. The part of plasma clearance related to kidney function can be determined as  $k_P = k_A - k_T$ . Therefore, we can calculate the GFR as follows

$$\text{GFR} = k_P \cdot V_D \tag{3}$$

$$k_P = k_A - k_T \tag{4}$$

where  $k_P$  is the rate constant of the plasma clearance of the marker molecule related to kidney function, and  $V_D$  is the distribution volume. As a first approximation,  $V_D$  equals the whole plasma volume. According to Eq. 3, it is equivalent to use plasma clearance rate or GFR for kidney function evaluation. Calculating GFR requires the knowledge of a distribution volume  $V_D$ , which varies from individual to individual and may also vary over time. The plasma clearance rate constant of a GFR marker molecule, on the other hand, is a more direct measure of kidney function and independent of blood volumes of individual animals, in other words independent of the size and weight variations of the animals one uses. Here, we directly compare the plasma clearance rate constants obtained in different animal experiments and show the compiled results of measured rate constants in Fig. 5. It should be pointed out that in a need of estimating GFR from plasma clearance

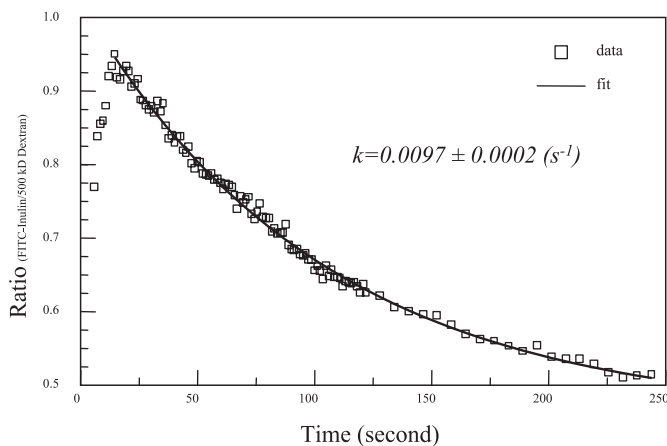


Fig. 4. Example of FITC-inulin plasma clearance curve measured from the blood plasma using intensity ratio. Open squares: data points; solid line: a fit to the elimination phase using Eq. 2. A single exponential fits the clearance phase data points very well, and the fitting curve goes through the initial points of the elimination phase as well as points at the tail.

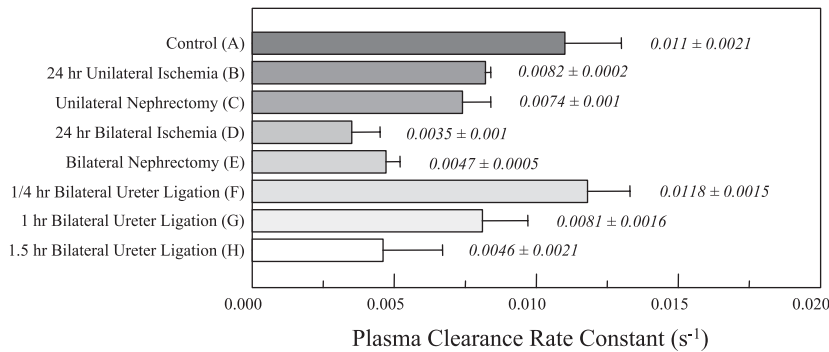


Fig. 5. Comparison between measured plasma clearance rate constants using the ratiometric imaging approach in different animal models with their kidney functions altered. A, controls. B, 24 h after a 30-min unilateral ischemia. C, unilateral nephrectomy. D, 24 h after a 30 min bilateral ischemia. E, bilateral nephrectomy. F, 15 min after bilateral ureter ligations. G, 1 h after bilateral ureter ligations. H, 1.5 h after bilateral ureter ligations. For A–E,  $n = 3$ . F, G, and H were measured from the same animal and each rate constant value  $k$  was an average from analyzing ratio data of 3 individual blood vessel regions.

measurements, typically the plasma volume can be calculated directly from the body weight (16) which is simple and practical. It is a common practice in the clinics to evaluate renal function by scaling the actual measurement results with body weights or surface areas.

From results in Fig. 5, by considering the nonrenal clearance rate constant  $k_T$  ( $\sim 0.0047 \text{ s}^{-1}$  obtained from the bilateral nephrectomy Fig. 5E), we can calculate GFR for an individual animal; e.g., we obtained  $\text{GFR} = 2.38 \pm 0.8 \text{ ml/min}$  for an animal of 229 g in body weight, with healthy kidneys, having a total plasma volume of 6.3 ml (50% of the total blood volume figured at 5.5% of the body weight) (1). In fact, this rate is close to the rate reported in the literature using magnetic resonance imaging techniques (20) to measure plasma clearance of a GFR marker. With the removal of one kidney, we obtained  $\text{GFR} = 1.34 \pm 0.5 \text{ ml/min}$  measured with a 302-g animal having a total plasma volume of 8.3 ml. This GFR value was  $\sim 56\%$  of that of the above-mentioned control animal, as one expected.

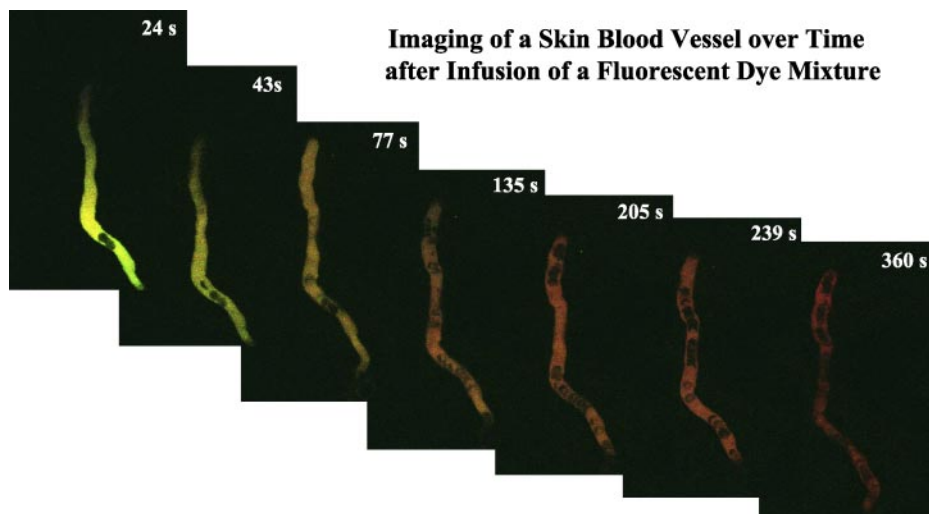
By using a bolus infusion of GFR markers, the nonspecific tissue distributions of the marker molecules contribute to the overall plasma disappearance kinetics of the marker molecules. This is a well-documented phenomenon and an issue associated with methods using plasma clearance to quantify renal filtration function. To remove this “nonrenal clearance” component, we have experimentally determined its kinetic rate constant by using a bilateral nephrectomy model. The fact that the rate constants of the nonrenal

clearance of the marker molecules are very close when renal filtration functions are stopped (Fig. 5, E and H) suggest that it has a well-defined value for the animal models we used. It should be noted that the nonrenal distribution rate is likely not a constant in different cases, such as in acute or chronic renal insufficiency, and should be investigated accordingly. However, in each one of these cases the corresponding renal plasma clearance rate constant still needs to be corrected using Eq. 4.

Alternatively, one can use a single exponential model with two rate constants to fit the overall kinetic curve and directly retrieve the rate constants of both the renal and nonrenal clearance of the marker molecules as follows

$$R_{\text{vessel}}(t) = A \exp[-(k_p + k_T)t] + C \quad (5)$$

where  $k_p$  and  $k_T$  are rate constants of renal and nonrenal plasma clearance, respectively, and  $A$  and  $C$  are constants. The use of a single expression (Eq. 5) and Eqs. 2 and 4 is mathematically equivalent. Typically, a multicompartiment model with double exponentials is used to account for the kinetics of GFR marker distribution in the blood volume after a bolus injection and the clearance of the marker molecules, respectively. Since we are using intensity ratio, the fraction of the distribution phase is negligible, and therefore what’s left is a single exponential term to account for the clearance kinetics. However, the overall rate constant of the clearance phase is a sum of individual rate constants of all processes contributing to the clearance kinetics. For a general case when the GFR marker distribution phase is



Imaging of a Skin Blood Vessel over Time after Infusion of a Fluorescent Dye Mixture

Fig. 6. Montage of color-combined fluorescence time-series images of a blood vessel from a rat skin area following a bolus infusion of a dye mixture. Green, FITC-inulin, Red, 500-kDa Texas red-dextran. The color of the blood vessel becomes increasingly red over time due to plasma clearance of FITC-inulin and increased fractional concentration of the 500-kDa Texas Red-dextran. Imaging was done on the rat penis. Image frame size is  $\sim 100 \times 150 \mu\text{m}^2$ .

present, the plasma clearance kinetics can be described as follows

$$R_{\text{vessel}}(t) = A \exp[-(k_p + k_T)t] + B \exp(-k_D t) + C \quad (6)$$

with  $k_T = \sum k_i$ ,  $k_i$  is the rate constant of any individual nonrenal clearance processes,  $k_D$  is the rate constant of marker distribution process, and  $A$ ,  $B$ , and  $C$  are constants. The use of a multicompartment model to fit the data and retrieve the plasma clearance rate constants can be helpful in human tests (4, 25) when the fraction of the distribution phase becomes more prominent.

*Inulin clearance rate measured by imaging the skin.* Since we measure the clearance rate of the marker molecule from the blood space, we should be able to determine the plasma clearance rate constant by making measurements at any bodily location wherever there is blood flow. To demonstrate that the plasma clearance rate constants measured by imaging the kidney represent renal function systemically, we performed in vivo kinetic imaging of plasma clearance on the skin. Figure 6 is a montage of color-combined intensity images of a skin blood vessel from a healthy male Sprague-Dawley rat. These images were acquired as a function of time following intravenous infusion of a FITC-inulin and 500-kDa Texas red-dextran mixture. Other than placement of a catheter in the vein, there were no surgeries involved. A skin area of male genitalia of the rat was imaged.

The clearance of FITC-inulin (in green) from the blood was visible as the green color gradually disappeared over time. At the end of 360 s after infusion, the fluorescent molecule left in the blood was mainly the 500-kDa Texas red-dextran (in red). The FITC-inulin-to-Texas red-dextran intensity ratio value of the whole blood vessel region was calculated from individual images and plotted as a function of time (Fig. 7). We obtained an inulin plasma clearance rate constant  $k = 0.0097 \pm 0.0010 \text{ (s}^{-1}\text{)}$  by fitting the data to Eq. 2. This rate constant value is almost identical to what was measured from imaging the kidney (Fig. 4). These results suggest there is no difference between imaging the kidney vasculature and imaging the skin in measuring inulin plasma clearance rates.

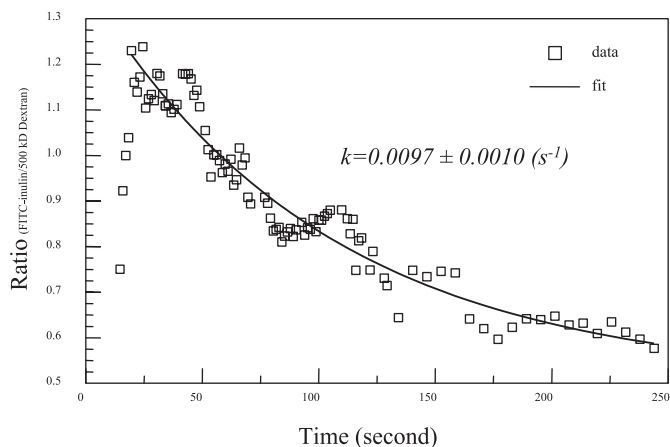


Fig. 7. Plasma clearance of FITC-inulin measured from within a blood vessel (same data set as in Fig. 6) as a function of time using the FITC-inulin-to-Texas red-dextran (500 kDa) intensity ratio. □, Data points. The solid line is a fit to the elimination phase using Eq. 2.

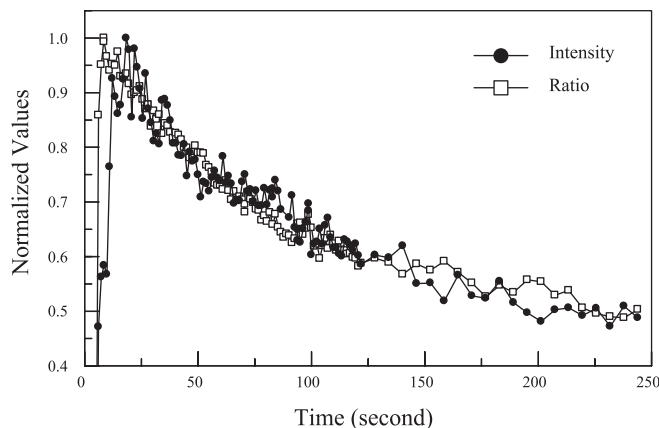


Fig. 8. Comparison between using FITC-inulin-to-500-kDa Texas red-dextran intensity ratio (□) and directly using FITC-inulin intensity alone (●). Both curves are normalized to their highest values, respectively. The peak of the intensity-alone curve is delayed with respect to the peak of the ratio curve. Other than that, both curves are significantly overlapped. The lines are used to guide the eyes.

In principle, plasma clearance rates can be measured at any bodily location where there is representative blood flow. We have experimented to image blood flow from the skin of the ear, using a skin flap (requires surgery), from the lips, and the genital areas of Sprague-Dawley rats. We found the genital area is relatively simple to image, involving fewer procedures to perform, not having the problem of the hair (highly fluorescent and a problem associated with imaging the ear), or interference with essential physiological functions (e.g., blocking or interfere with the airway, a problem in imaging

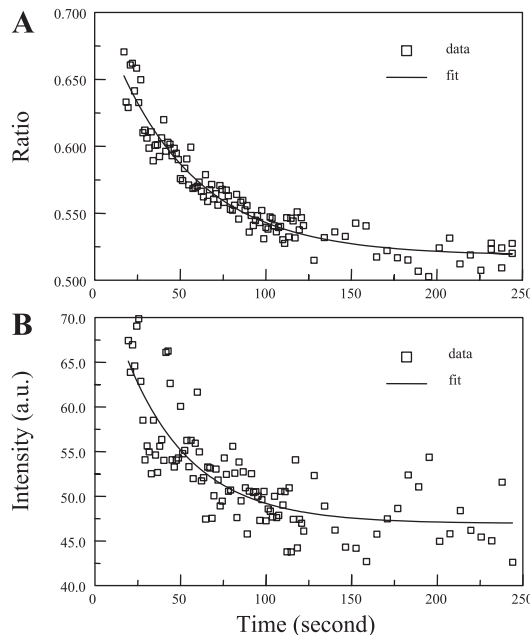


Fig. 9. Example showing that the intensity-alone data can be very noisy and the points are scattered, but the ratio data points are much tighter with a well-defined clearance curve. A: 3-kDa tetramethylrhodamine (TMR)-dextran-to-500-kDa FITC-dextran intensity ratio. B: 3-kDa TMR-dextran intensity alone. In this case, a mixture of 1.6 mg of the 3-kDa TMR-dextran and 1.6 mg of the 500-kDa FITC-dextran dissolved in 0.5 ml saline was used for infusion. The solid fit lines in both A and B are for guiding the eyes.

the lips). Imaging the genitalia of the animal allows us to directly experiment with the Sprague-Dawley model commonly used for different studies e.g., ischemia, without needing to use special animals such as the nude rats.

*Using intensity from a single probe vs. intensity ratio from two probes.* After fluorescent molecules are intravenously infused into the animal, they will distribute in the plasma and eventually reach concentration equilibrium. This dye distribution process usually requires a given period of time to complete. However, on the other hand, the filtration function of kidneys is a continuous function. At the moment a GFR marker molecule is being injected into the bloodstream, it is filtered by the kidneys almost instantaneously on reaching the kidney glomeruli. As a result of this kinetic process, if one uses the signal from a single GFR marker, the kinetics of plasma distribution and plasma clearance processes are convoluted. Different from using intensity values from a single source, by infusing two probes at the same time, the initial plasma distributions of the two molecules happen at the same time and the contribution, due to plasma distribution, to the overall kinetic signals is minimized using the ratio values of one probe being filtered and the other being retained in the blood. This difference is illustrated in Fig. 8. The fluorescence intensity value (from FITC-inulin) peaked at  $\sim 20$  s (Fig. 8) after infusion was significantly delayed compared with the time when the ratio value reached its peak (at  $\sim 7$  s). At 20 s postinfusion, FITC-inulin had already been filtered and present in the proximal tubular lumen for  $>10$  s (Fig. 1). Clearly, the kinetic curve using FITC-inulin intensity (Fig. 8) alone misaligns in time with the filtration process. As a result, the initial data points were either not acquired or not used for retrieving the rate constants of plasma clearance using signals from single GFR markers alone (16). On the contrary, the peak of the kinetic curve using intensity ratio data (Fig. 8) matches more closely the appearance of dextran mixture in the renal peritubular capillaries (usually within the time period of acquiring one image frame, which is 1.22 s under our experimental conditions). Therefore, the initial data points related to the (plasma) clearance phase can be used for curve fitting using a single exponential. Consequently, the decay trace using intensity ratio data better represents the kinetics of plasma clearance, simplifies the mathematical model used for fitting, and allows rapid renal function analysis.

In addition, a comparison of the kinetic data between using the intensity ratio and directly using the intensity value of a 3-kDa tetramethylrhodamine-conjugated dextran (3-kDa TMR-dextran) alone is shown in Fig. 9. The differences include the following.

1. The intensity fluctuation of the 3-kDa TMR-dextran alone was quite significant (Fig. 9B). Consequently, the fitting result of the clearance rate constant contains larger errors ( $>15\%$ ) and is less defined. In contrast, the intensity ratio (between 3-kDa TMR-dextran and 500-kDa FITC-dextran) has significantly less noise, and the measured clearance rate constant is much better defined with significantly less error. This is partially because fluorescence intensity is typically very sensitive to even a slight change in focus and movement of the sample. Intensity ratio, on the other hand, is insensitive to minor changes in imaging depth and motion. We are focusing on the fluorescence signals from the blood. The intensity signal of a dye from the blood can change when the blood flow rate

changes. However, the relative intensity ratio between two molecules does not change even when the blood flow rate or blood volume changes (assuming there is no clearance). This is because both dye molecules are present in the blood and move together.

2. As discussed earlier, the separation between the initial dye distribution and the clearance phase is well defined using the intensity ratio. In the case of using the intensity of a single dye alone, it is more difficult to determine at what time point the clearance phase begins. The highest data point in the intensity curve typically does not correlate in time with the appearance of the smaller molecule in the proximal tubule lumen. Therefore, the dye distribution and the filtration phases are convoluted in the intensity only curve (16, 21). If we fit the data using the same model as the one to which we fit the ratio curve, we may miscalculate the plasma clearance rate.

Although the data shown in Figs. 8 and Fig. 9 are results using a fluorescent GFR marker, the associated disadvantages of using the signals from single marker molecules exist in other plasma clearance-based GFR measurement techniques, when single nonfluorescent marker molecules, e.g.,  $[^{125}\text{I}]$ iothalamate, technetium-labeled diethylenetriamine penta-acetate, or  $^{51}\text{Cr}$ -EDTA, are used. In these cases when ratios are not used, one has to apply more complicated models to describe the whole plasma clearance kinetics to retrieve the clearance rate constant of the marker molecules.

In conclusion, as demonstrated in the animal experiments, the ratiometric microscopic imaging technique we have developed provides a quantitative means for determining kidney function with improved accuracy and sensitivity compared with techniques using signals from single GFR marker molecules alone. Consequently, it allows rapid evaluations of kidney function and as a result the initial data points of the clearance phase immediately postinfusion can be used effectively with a simple mathematical model, which provides a tool for quantifying renal function even when it is severally reduced. This ratiometric technique eliminates the need for continuous infusion, urine collection, and other procedures used for measuring renal function, and it can be also applied to improve other techniques used to determine glomerular filtration function based on plasma disappearance rates.

#### ACKNOWLEDGMENTS

The authors thank Dr. Silvia B. Campos for performing animal surgeries, Xianming Chen and Ashley M. Dutton for technical support, and the Indiana Center for Biological Microscopy for using its microscopic imaging facility. The authors also thank Drs. Timothy Sutton, Pierre Dagher, and Robert Bacallao for support and stimulating discussions.

#### GRANTS

This work was supported by startup funds from an Indiana Genomics Initiative (INGEN) Grant from the Eli Lilly and Company Foundation to the Indiana University School of Medicine (W. Yu) and a pilot study fund from an National Institutes of Health (NIH) O'Brien Center of Excellence Grant (W. Yu). The Indiana Center for Biological Imaging is supported by grant funds from INGEN and an NIH O'Brien Center of Excellence Award (P50 DK-61594) to B. A. Molitoris.

#### REFERENCES

1. Altman P. Blood volumes of mammals. In: *Blood and Other Body Fluids* (1st ed.), edited by Dittmer DS. Washington, DC: FASEB, 1961, p. 3–5.

2. **Bevington PR.** *Data Reduction and Error Analysis for the Physical Sciences* (1st ed.). New York: McGraw-Hill, 1969.
3. **Centonze VE, White JG.** Multiphoton excitation provides optical sections from deeper within scattering specimens than confocal imaging. *Biophys J* 75: 2015–2024, 1998.
4. **Cousins C, Mohammadtaghi S, Mubashar M, Strong R, Gunasekera RD, Myers MJ, Peters AM.** Clearance kinetics of solutes used to measure glomerular filtration rate. *Nucl Med Commun* 20: 1047–1054, 1999.
5. **Dagher PC, Herget-Rosenthal S, Ruehm SG, Jo SK, Star RA, Agarwal R, Molitoris BA.** Newly developed techniques to study and diagnose acute renal failure. *J Am Soc Nephrol* 14: 2188–2198, 2003.
6. **Dunn KW, Sandoval RM, Kelly KJ, Dagher PC, Tanner GA, Atkinson SJ, Bacallao RL, Molitoris BA.** Functional studies of the kidney of living animals using multicolor two-photon microscopy. *Am J Physiol Cell Physiol* 283: C905–C916, 2002.
7. **Dunn KW, Sandoval RM, Molitoris BA.** Intravital imaging of the kidney using multiparameter multiphoton microscopy. *Nephron Exp Nephrol* 94: e7–e11, 2003.
8. **Erley CM, Bader BD, Berger ED, Vochazer A, Jorzik JJ, Dietz K, Risler T.** Plasma clearance of iodine contrast media as a measure of glomerular filtration rate in critically ill patients. *Crit Care Med* 29: 1544–1550, 2001.
9. **Kang JJ, Toma I, Sipos A, McCulloch F, Peti-Peterdi J.** Quantitative imaging of basic functions in renal (patho)physiology. *Am J Physiol Renal Physiol* 291: F495–F502, 2006.
10. **Kelly KJ, Williams WW Jr, Colvin RB, Meehan SM, Springer TA, Gutierrez-Ramos JC, Bonventre JV.** Intercellular adhesion molecule-1-deficient mice are protected against ischemic renal injury. *J Clin Invest* 97: 1056–1063, 1996.
11. **Kim SJ, Lim YT, Kim BS, Cho SI, Woo JS, Jung JS, Kim YK.** Mechanism of reduced GFR in rabbits with ischemic acute renal failure. *Ren Fail* 22: 129–141, 2000.
12. **Molitoris BA, Sandoval R, Sutton TA.** Endothelial injury and dysfunction in ischemic acute renal failure. *Crit Care Med* 30: S235–240, 2002.
13. **Molitoris BA, Sandoval RM.** Intravital multiphoton microscopy of dynamic renal processes. *Am J Physiol Renal Physiol* 288: F1084–F1089, 2005.
14. **Peti-Peterdi J, Morishima S, Bell PD, Okada Y.** Two-photon excitation fluorescence imaging of the living juxtaglomerular apparatus. *Am J Physiol Renal Physiol* 283: F197–F201, 2002.
15. **Peti-Peterdi J, Fintha A, Fuson AL, Tousson A, Chow RH.** Real-time imaging of renin release in vitro. *Am J Physiol Renal Physiol* 287: F329–F335, 2004.
16. **Qi Z, Whitt I, Mehta A, Jin J, Zhao M, Harris RC, Fogo AB, Breyer MD.** Serial determination of glomerular filtration rate in conscious mice using FITC-inulin clearance. *Am J Physiol Renal Physiol* 286: F590–F596, 2004.
17. **Rabito CA, Moore RH, Bougas C, Dragotakes SC.** Noninvasive, real-time monitoring of renal function: the ambulatory renal monitor. *J Nucl Med* 34: 199–207, 1993.
18. **Rabito CA, Panico F, Rubin R, Tolokoff-Rubin N, Teplick R.** Noninvasive, real-time monitoring of renal function during critical care. *J Am Soc Nephrol* 4: 1421–1428, 1994.
19. **Sandoval RM, Kennedy MD, Low PS, Molitoris BA.** Uptake and trafficking of fluorescent conjugates of folic acid in intact kidney determined using intravital two-photon microscopy. *Am J Physiol Cell Physiol* 287: C517–C526, 2004.
20. **Seshan V, Germann MJ, Preisig P, Malloy CR, Sherry AD, Bansal N.** TmDOTP5- as a <sup>23</sup>Na shift reagent for the in vivo rat kidney. *Magn Reson Med* 34: 25–31, 1995.
21. **Sturgeon C, Sam AD, 2nd, Law WR.** Rapid determination of glomerular filtration rate by single-bolus inulin: a comparison of estimation analyses. *J Appl Physiol* 84: 2154–2162, 1998.
22. **Sutton TA, Fisher CJ, Molitoris BA.** Microvascular endothelial injury and dysfunction during ischemic acute renal failure. *Kidney Int* 62: 1539–1549, 2002.
23. **Sutton TA, Mang HE, Campos SB, Sandoval RM, Yoder MC, Molitoris BA.** Injury of the renal microvascular endothelium alters barrier function after ischemia. *Am J Physiol Renal Physiol* 285: F191–F198, 2003.
24. **Sutton TA, Kelly KJ, Mang HE, Plotkin Z, Sandoval RM, Dagher PC.** Minocycline reduces renal microvascular leakage in a rat model of ischemic renal injury. *Am J Physiol Renal Physiol* 288: F91–F97, 2005.
25. **Swinkels DW, Hendriks JC, Nauta J, de Jong MC.** Glomerular filtration rate by single-injection inulin clearance: definition of a workable protocol for children. *Ann Clin Biochem* 37: 60–66, 2000.
26. **Tanner GA, Sandoval RM, Dunn KW.** Two-photon in vivo microscopy of sulfonefluorescein secretion in normal and cystic rat kidneys. *Am J Physiol Renal Physiol* 286: F152–F160, 2004.
27. **Williams P, Lopez H, Britt D, Chan C, Ezrin A, Hottendorf R.** Characterization of renal ischemia-reperfusion injury in rats. *J Pharmacol Toxicol Methods* 37: 1–7, 1997.
28. **Yu W, Sandoval RM, Molitoris BA.** Quantitative intravital microscopy using a Generalized Polarity concept for kidney studies. *Am J Physiol Cell Physiol* 289: C1197–C1208, 2005.
29. **Yu W.** Quantitative microscopic approaches for studying kidney functions. *Nephron Physiol* 103: p. 63–70, 2006.